Experimental Investigation on Convective Heat Transfer Characteristics in Ribbed Channel

Xie Changtan[1], *Xue Shulin*[1], *Yang Weihua*[2*]

1. AEEC Hunan Avation Powerplant Research Institute, Zhuzhou 412002, P. R. China;
2. College of Energy and Power Engineering, Nanjing University of Astonautics and Aeronautics, Nanjing 210016, P. R. China

(Received 2 November 2017; revised 16 January 2018; accepted 20 January 2018)

Abstract: The heat transfer and pressure loss characteristics on a square channel with two opposite surfaces roughened by high blockage ratio ribs are measured by systematic experiments. Reynolds numbers studied in the channel range from 1 400 to 8 000. The ratios of rib height to hydraulic diameter (e/D) are 0.2 and 0.33, respectively. The ratio of rib spacing to height(P/e) ranges from 5 to 15. The rib orientations in the opposite surfaces are symmetrical and staggered arrangements. The results show that the heat transfer coefficients are increased with the increase of rib height and Reynolds number, though at the cost of higher pressure losses. When the rib spacing to height ratio is 10, it keeps the highest heat transfer coefficient in three kinds of rib spacing to height ratios 5, 10 and 15. The heat transfer coefficient of symmetrical arrangement ribs is higher than that of the staggered arrangement ribs, but the pressure loss of the symmetrical arrangement ribs is larger than that of the staggered arrangement ribs.

Key words: convective heat transfer; rib channel; experimental investigation; aeroengine

CLC number: V231.1 **Document code**: A **Article ID**: 1005-1120(2018)06-0962-11

Nomenclature

A	[m^2]	Heat area of stainless foil
D	[m]	Hydraulic diameter
h	[$W/m^2 \cdot K$]	Heat transfer coefficient
L	[m]	Length
p	[Pa]	Pressure
Q	[W]	Heat flow of stainless foil
T	[K]	Temperature
u	[m/s]	Flow velocity

Special characters

ε	[-]	Surface emissivity
σ	[m]	Stefan-boltzmann constant
ρ	[kg/m^3]	Density
λ	[W/mK]	Thermal conductivity
υ	[m^2/s]	Kinematic viscosity

Subscripts

a	Air
amb	Ambient
c	Convection
in	Inlet
out	Outlet
ow	Outside wall
rad	Radiation
w	Wall

0 Introduction

Advanced gas turbine engines operate at high temperature to improve thermal efficiency and power output. As the turbine inlet temperature increases, the heat transferred to the turbine blades also increases. The level and variation in the temperature within the blade material must be limited to achieve reasonable durability goals. Because the operating temperature of modern gas turbines is far above the permissible metal temperature, there is a need to cool the blade for safe operation. There are two methods used for turbine blades to protect the blade material from ex-

* Corresponding author, E-mail address: Yangwh@nuaa.edu.cn.

How to cite this article: Xie Changtan, Xue Shulin, Yang Weihua. Experimental investigation on convective heat transfer characteristics in ribbed channel[J]. Trans. Nanjing Univ. Aero. Astro., 2018,35(6):962-972.
http://dx.doi.org/10.16356/j.1005-1120.2018.06.962

ceeding the maximum allowable temperature, one is external cooling, such as film cooling, and the other is internal cooling, such as impingement cooling, rib turbulated cooling, and pin-fin cooling. The internal cooling is achieved by passing the coolant through several enhanced serpentine passage inside the blade and extracting the heat from the outside of the blades. A common method of increasing the cooling capacity of the internal cooling circuit is the addition of rib turbulators to the internal coolant channel walls. The addition of the rib turbulators increases the overall internal convective heat transfer coefficient, causing a corresponding drop in the component metal temperature.

Over the last few decades, there have been many studies on configuration parameters, such as rib shape, aspect ratio, pitch ratio, blockage ratio e/Dh, rib angle of attack, and so on[1-6]. Refs. [7-11] studied the effect of Reynolds number on the centerline heat transfer coefficient of a square channel ($W/H=1$) and two rectangular channels ($W/H=2,4$) for two rib spacing($P/e=10,20$). The heat transfer distribution was presented by a Nusselt number ratio with several Reynolds numbers, and they showed similar trends except that the Nusselt number ratios decreased slightly with increasing Reynolds numbers. Refs. [12,13] figured out that the best rib pitch to height ratio is between 7 and 15. Ref. [14] experimentally studied the heat transfer characteristics for 90° rib turbulator. They found that the internal rib turbulator can increase the overall effectiveness on the vane external surface by up to 50% relative to the non-ribbed model. Ref. [15] experimentally investigated the conjugate heat transfer in a rib-roughened trailing edge channel with crossing jets. The cooling scheme is characterized by a trapezoidal cross-section, one rib-roughened wall, and slots along two opposite walls. The Reynolds number is set at 67 500 for all the experiments. The measurements are performed using three different ribbed walls, with thermal conductivities ranging from 1 W/(m·K) to 18 W/(m·K). They found that the levels of the Nusselt number obtained in the purely convective regime (uniform heat flux at the wall-fluid interface) are off by up to 30% locally and 25% globally with respect to the conjugate results. Ref. [16] studied the flow and heat transfer characteristics in rectangular rib-roughened passages. They found that the side-wall heat transfer coefficients of the passage with ribs on opposite walls are about 20%—43% higher than that of a smooth passage, and the length of the ribs affects the heat transfer and friction characteristics. The level of augmentation of heat transfer becomes higher as the Reynolds number increases. Ref. [17] investigated the effects of P-type and V-type rib arrangements on the flow pattern and heat transfer in an internally ribbed heat exchanger tube. The results revealed that the average Nusselt number and friction factor in the V-type ribbed tubes were about 57%—76% and 86%—94% higher than those in the P-type ribbed tube, respectively. The performance evaluation criterion (PEC) based on the same pumping power in the V-type ribbed tube varied from 1.32 to 1.74, which was about 27%—41% higher than that in the P-type ribbed tube. Ref. [18] investigated the turbulent flow and heat transfer behaviour in the rectangular channel with inclined broken ribs for three kinds of rib arrays. They claimed that the heat transfer of the inclined broken ribbed channel was improved about 160%—230% compared with smooth duct because of the generation of co-rotating longitudinal vortices. Ref. [19] evaluated the heat transfer performance in a rectangular channel of sixteen types of rib shapes, and they found that boot-shaped rib design showed the best heat transfer performance with a pressure drop similar to that of the square rib. Ref. [24] studied the flow and heat transfer characteristics in a two-pass 90° ribbed parallelogram channel with infrared thermography and particle image velocimetry. It is found that the flow dynamic mechanisms responsible for the rib top and mid-rib heat transfer enhancement are different for the inlet and outlet passes. The presences of a high Nu_0 streak between the last inlet-leg rib and the bend as well as

two high Nu_0 zones inside the bend are the new found features lacking in the corresponding two-pass 90° ribbed square channel. In addition, simple correlations of Nu_0 and f_0 with Re are acquired. Thermal performance factors are about 66% and 28% higher than the previous reported smooth-walled counterpart at $Re = 5\ 000$ and 20 000, respectively. Ref. [25] studied the effects of inlet velocity profile on flow and heat transfer in the entrance region of a ribbed channel. They found that in the entrance region, the location and shape of the reattachment and the recirculation region were altered by the local velocity distribution caused by the different inlet velocity profiles. Therefore, the distribution and the strength of the vorticity in the channel were changed, and the local heat transfer coefficient and pressure drop in the channel were affected by the inlet velocity profile.

From the above we can know that the flow and heat transfer characteristics of rib-roughened channels have been deeply studied by a lot of researchers in the last few decades. Almost all studies in open literatures focus on higher Reynolds number (8 000 at least) and a lower blockage ratio(5%—10%). However, for the smaller gas turbine, the turbine blades have higher blockage ribs and lower coolant Reynolds number at closer spacing of turbine blade. The objective of this study is to measure heat transfer coefficient and friction factor for a 90° parallel rib-roughened high blockage ($0.2 < e/D < 0.33$) square channel with pacing (P/e) ranging from 5 to 15. The tested Reynolds numbers are between 1 400 and 8 000. The study results are the benefit supplement for the internal cooling design of turbine blades.

1 Experimental Setup

Fig. 1 shows the comprehensive scheme of experimental setup. It consists of compressor, buffer tank, mass flow controller and test section. The air from compressor with environment temperature is ducted into the test section. A ball valve is provided upstream of the test section to protect and control the flow rate. The flow is measured using a mass flow controller. The temperature of the air flowing into the test section is monitored by a T-type thermocouple. The spent air from the test section is directly exhausted into the atmosphere. The accuracy of the mass flow controller and the T-type thermocouple is 1.0% and ±0.1 ℃, respectively. The temperature of the test wall (heating foil) is measured by an infrared thermography system TVS-2000MK with accuracy of ±0.4℃ and measured temperature range of −40—2 000 ℃. All the measurement data of temperature are connected with a 8-channel HP34970A data collection system.

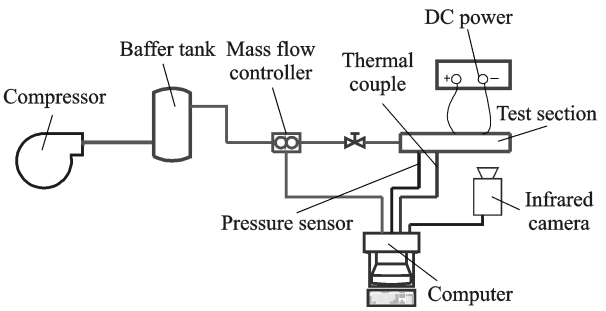

Fig. 1 Experimental setup

Fig. 2 is the schematic of the test section. There are two kinds of test sections in this experiment. Both the test sections are rectangular channels. The geometrical dimensions of the test sections are 180 mm(length)×60 mm(width)×15 mm(height) and 180 mm(length)×60 mm(width)×9 mm(height), respectively. At the entrance of the test section, there are a T-type thermocouple and a static pressure probe to measure the temperature and the static pressure of stream. The heating foil with uniform heat flow provided by direct current heating is made of stainless steel foil with thickness of 0.02 mm and size of 180 mm(length)×60 mm(width), which is glued on the insulate plate of the test section. The surface of heating foil is painted with black paint to assure a uniform emissivity of 0.96. The channels are roughened with square cross section ribs made of stainless steel. The width, height

and length are 3, 3 and 60 mm, respectively. All the ribs are glued on the heating foil and the infrared grass in accordance with the test requirements. The ribs on the opposite wall are laid parallel to each other and placed with a given spatial periodicity. The temperature of the heating foil is measured by infrared camera. In order to measure the complete temperature field of the rib roughened heating foil, it needs to measure the temperature field from three angles with the infrared camera. Three T-type thermocouples are fixed on the back of stainless steel foil with 502 glue as the reference for the infrared thermograph system.

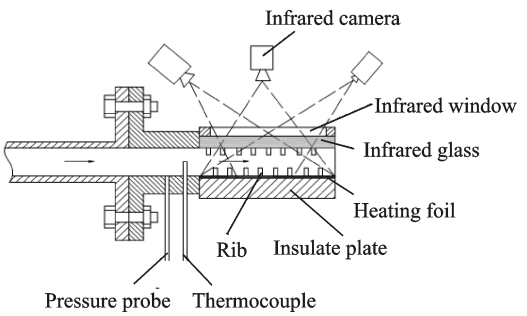

Fig. 2 Schematic of test section

The relationship between corrected infrared temperature and thermocouple date is

$$T = -13.6 + 1.46T_0 - 0.005\ 28T_0^2 \quad (1)$$

where T_0 is the infrared thermograph temperature, and T is the corrected infrared temperature.

The insulated plate to minimize ambient heat transfer loss is made of a 20 mm thick Bakelite slab, which has a very low thermal conductivity of 0.06 W/(m·℃). Three T-type thermocouples are glued on the outside of the insulated plate.

There are two kinds of rib arrangements for the rib roughened channel, one is symmetrical arrangement, and the other is staggered arrangement. The geometry dimensions of rib roughened channels are shown in Fig. 3 and Table 1.

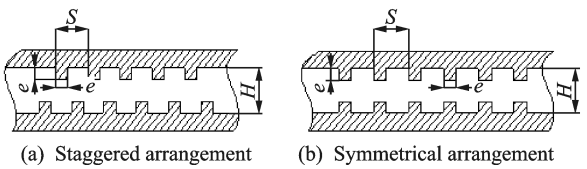

Fig. 3 Schematic of rib arrangements

Table 1 Geometry dimensions of rib roughened channel

Rib arrangement	e	H	P	P/e	e/D
Symmetrical arrangement	3	15	15	5	0.2
			30	10	
			45	15	
	3	9	15	5	0.33
			30	10	
			45	15	
Staggered arrangement	3	15	15	5	0.2
			30	10	
			45	15	
	3	9	15	5	0.33
			30	10	
			45	15	

2 Data Reduction

The Reynolds number is computed using

$$Re = \frac{uD}{\nu} \quad (2)$$

where u is the inlet velocity of the test section, which is computed from the mass flow rate calculated from the mass flow controller. D is the inlet hydraulic diameter of the test section, and ν is the kinematic viscosity.

The heat transfer coefficient h is estimated as

$$h = \frac{Q - Q_{loss}}{A(T_w - T_a)} \quad (3)$$

where $Q = UI$ is the heat flow of stainless foil when the foil is being heated by passing DC power which has the accuracy of ±0.1 V and ±0.1 A for voltage U and electric current I, respectively. A is the heat area of stainless foil. As the desired voltage V and current I passing through the test plate, the heat flux Q along the surface of stainless foil can be calculated. T_w is the wall temperature of stainless foil heated by passing DC power. T_a is the air temperature at the inlet section of the test section which can be measured by the T-type thermocouple. $Q_{loss} = Q_{con} + Q_{rad}$ is the heat loss from the outer surface of the insulted plate to ambient, which includes natural convection heat loss Q_{con} and radiation heat loss Q_{rad}. The natural convection heat loss Q_{con} is calculated by

$$Q_{con} = Ah_{nat}(T_{ow} - T_{amb}) \quad (4)$$

where T_{ow} is the outer surface temperature of the insulated plate, T_{amb} is the ambient temperature,

and h_{nat} is the natural convection heat transfer coefficient which can be obtained in Ref. [26].

$$Nu_{nat} = 0.59(GrPr)^{0.25} \tag{5}$$

where Gr and Pr are the Grashof number and Prandtl number, respectively.

The radiation heat loss Q_{rad} is calculated by

$$Q_{loss} = \sigma\varepsilon A(T_w^4 - T_{amb}^4) \tag{6}$$

where $\sigma = 5.67 \times 10^{-8}$ W/(m^{2}K^4) is the Stefan-Boltzmann constant, and $\varepsilon_{ow} = 0.6$ is the outer surface emissivity of the insulated plate.

The temperature distribution on the surface of stainless foil (heated or unheated) is recorded by an infrared thermography system operating in the middle IR band (8—14 μm) of the infrared spectrum. The temperature calculation method of the temperature map obtained from the infrared thermography system was described in Ref. [27]. In all of the experiments, the outer surface temperature of the insulated plate is between 25.5 ℃ and 25 ℃ while ambient temperature is approximately 24 ℃. The difference between ambient temperature and outer surface temperature of the insulated plate is less than 1.5 ℃. So, the natural convection heat loss is about 0.1 W, the radiation heat loss is about 0.145 W, and the total heat loss Q_{loss} is about 0.245 W which is far less than the heat flow Q. Thus, it is reasonable to ignore the heat loss from the outer surface of the insulated plate.

The average Nusselt number is defined as

$$Nu = \frac{hD}{\lambda} \tag{7}$$

where λ is the thermal conductivity of the air.

The friction factor is defined as

$$f = 2\frac{D}{\rho u^2}\frac{p_{in} - p_{out}}{\Delta L} \tag{8}$$

where p_{in} and p_{out} are the pressures of the inlet and outlet sections of the test section. The average inlet velocity u is calculated using the channel mass flow rate and ΔL is the length of ribbed segment of the test section.

The smooth channel correlations of Dittus-Boelter and Moody are utilized for normalizing the ribbed channel data. The classical Dittus-Boelter correlation is

$$Nu_0 = 0.023Re_f^{0.8}Pr_f^{0.4} \tag{9}$$

According to Ref. [28], experimental uncertainties in average Nusselt number, friction factor measurement were estimated to be about ±9.5% and ±6.3%, respectively. The individual uncertainty in air stream temperature T_a was ±0.4 ℃ and heating foil temperature T_w was ±0.1 ℃.

3 Results and Analysis

In the experiment, it is very difficult to precisely control the flow. Thus, the Reynolds number of different experimental sections cannot keep the same.

Fig. 4 shows the effect of rib spacing on Nusselt number for staggered and symmetrical rib channels. It can be seen that the rib pitch-to-height ratio has a large effect on the heat transfer coefficient of rib roughened channel. Whether the ribs are symmetrical or staggered, the rib height ratio equal to 10 corresponds to the maximum heat transfer coefficient. Clearly, for symmetrical ribbed channel and staggered ribbed channel, the heat transfer coefficient corresponding to rib height ratio equal to 15 is the smallest. The heat transfer coefficient of rib pitch-to-height ratio equal to 5 is between $S/e = 10$ and 15. This indicates that, for the ribbed channels with larger blockage ratio (0.33, 0.2), the influence of rib spacing on heat transfer coefficient does not increase monotonously with the increase of rib spacing, but there exists an optimal rib pitch to height ratio. The optimum pitch to height ratio in the experiment is 10. This conclusion is the same as that in Refs. [12,13]. At the same time, it also can be seen clearly that the heat transfer coefficient linearly increases with the increase of Reynolds number. In general, the main reasons for the enhancement of convective heat transfer in the rib roughened channel are the flow separation vortices behind the rib and the reattachment of the rib wall (Fig. 5). However, as the increase of the rib pitch, the effects of separation vortex and reattachment on the convective heat transfer are weaker and weaker, but the effect of flowing over a flat region after the reattachment region on con-

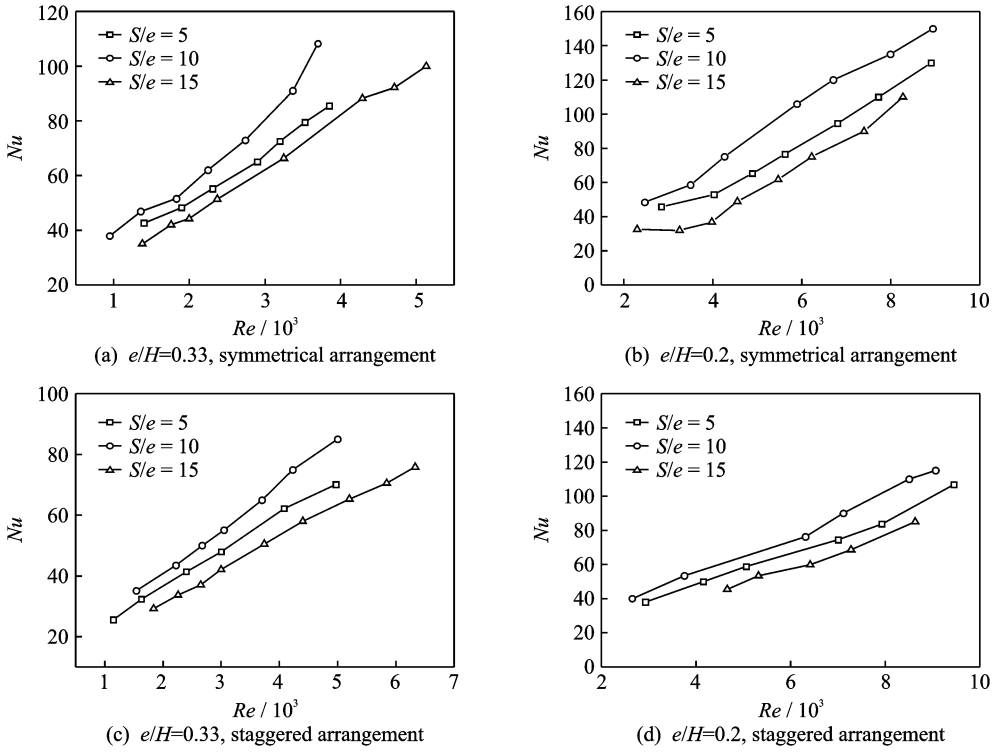

Fig. 4 Effect of rib pitch-to-height ratio P/e on Nu

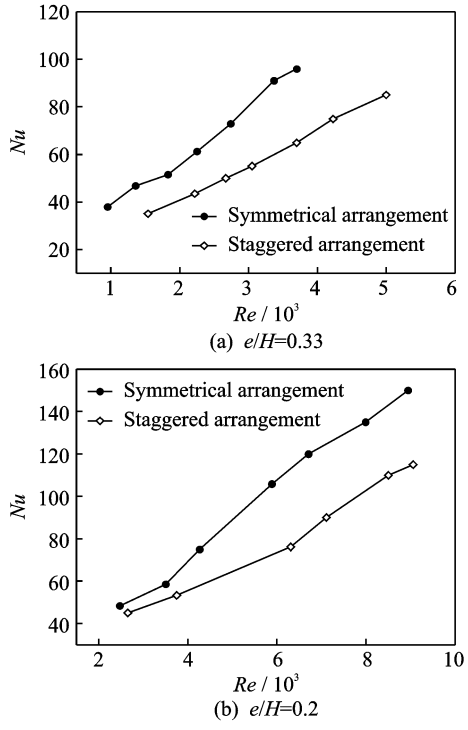

Fig. 5 Effect of rib arrangement on Nu

vective heat transfer is increased gradually. When rib spacing is large enough ($S/e=15$), the convective heat transfer of flow over flat is the main reason influencing on the convective heat transfer in the ribbed channel, resulting in a lower convective heat transfer coefficient. On the other hand, the flow reattachment to the rib wall will be gradually weakened as the decrease of rib pitch. When the rib pitch is small enough ($S/e=5$), the phenomena of flow reattachment will be disappeared, which also results in a lower heat transfer coefficient in the rib roughened channel. Thus, only when the rib spacing is appropriate ($S/e=10$) in ribbed channel, both of the flow separation vortex and reattachment to rib wall can play main roles on the convective heat transfer, leading to an optimal convective heat in the rib roughened channel.

Fig. 5 shows the effect of rib arrangement on the heat transfer coefficient for the blockage ratios $e/H=0.33$ and 0.2 when $P/e=10$. The plotted results show that rib arrangement has a larger effect on the heat transfer coefficient of rib-roughened channel. In general, the average Nusselt number of symmetrical ribs is higher than that of staggered ribs. However, the difference of Nusseult number between symmetrical ribs and staggered ribs is different for different blockage ratios

e/H. It is increased with the increasing of blockage ratio e/H. The difference of Nusseult number for $e/H=0.33$ is larger than that for $e/H=0.2$.

Fig. 6 shows the effect of rib blockage ratio on heat transfer coefficient when $S/e=10$. It can be seen that there is a large effect for the blockage ratio on the heat transfer coefficient. In general, a larger blockage ratio in the ribbed channel corresponds to a higher heat transfer coefficient. So, the heat transfer coefficient of blockage ratio $e/H=0.33$ is higher than that of blockage ratio $e/H=0.2$. However, because of the difference of rib arrangements, the difference of heat transfer coefficient between the two blockage ratios is also different. Clearly, the difference of heat transfer coefficient for the symmetrical rib arrangement is higher than that for the staggered rib arrangement. The reason to explain this kind of phenomena is that whether symmetrical rib channel or staggered rib channel, the flow disturbance in the rib channel with $e/H=0.33$ is significantly higher than that in the rib channel with $e/H=0.2$, which results in a larger heat transfer coefficient for the rib channel with $e/H=0.3$.

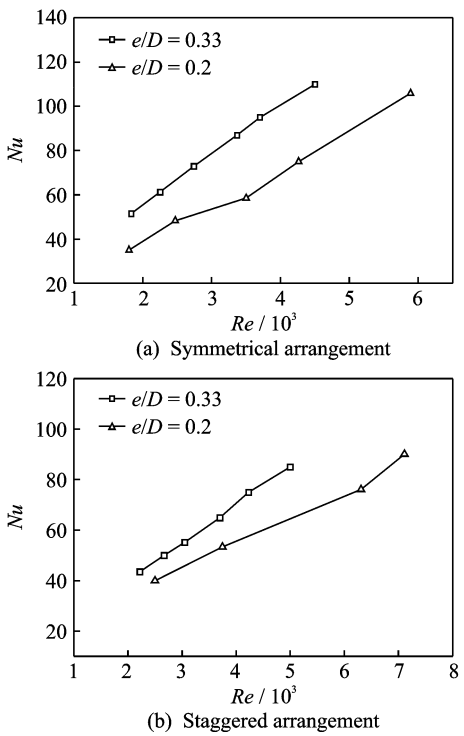

Fig. 6 Effect of blockage ratio on heat transfer coefficient

Fig. 7 shows the comparison of heat transfer coefficient between one-side rib channel and two-side rib channel. Clearly, the heat transfer coefficient of two-side rib channel is distinct higher than that of one-side rib channel. The difference is increased with increasing flow Reynolds number, which is from the smallest value 10 at the $Re=3\ 000$ up to the largest value 60 at the $Re=9\ 000$. The reason for this phenomena is that both of the flow separation vortexes and reattachment to the heat wall in the one-side rib channel are distinct weaker than that in two-side rib channel, thus the disturbance in the one-side rib channel is far less than that in the two-side rib channel, which results in a weaker turbulent mixing

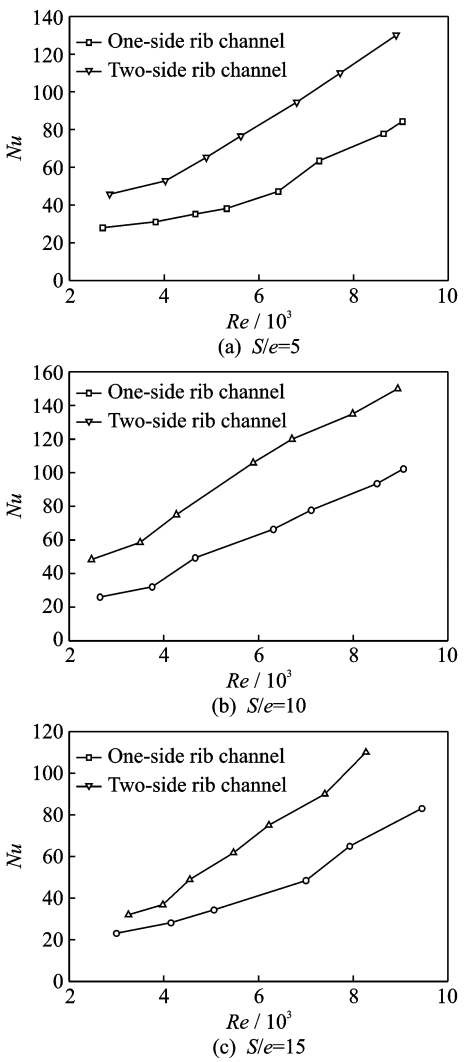

Fig. 7 Comparison of heat transfer coefficient between one-side and two-side rib channels with staggered arrangement

in one-side rib channel than that in two-side rib channel. So, the heat transfer coefficient of two-side ribbed channel is distinct larger than that of one-side ribbed channel.

Fig. 8 shows the average Nusselt number ratio Nu/Nu_0 for all different ribbed channels as a function of the Reynolds number. Nu_0 is the Nussult number of smooth channel. In general, when the fluid flows through smooth tube, if $Re<2\ 300$, it is a laminar flow; if $Re>2\ 300$, it is a turbulent flow. Thus, when $Re<2\ 300$, Nu_0 for fully developed laminar flow in duct is 6.1[29]. When $Re>2\ 300$, Nu_0 can be obtained by Eq. (9). So, the average Nusselt number ratio curves are divided into two regions, one is a laminar region, the other is a turbulent region. It can be observed that there exists a large difference for the heat transfer enhancement in the two regions. In the laminar region, the heat transfer enhancement rapidly increases with the increasing Reynolds number. For the symmetrical rib channel, as the increase of the Reynolds numbers from 1 000, 1 400, and 1 300 to 2 250, 2 300 and 2 000, the heat transfer enhancements are about 6—10 times, 7—9 times and 5.5—7 times for the ribbed channel with $S/e=10$, 15, and 5 , respectively, compared with the smooth duct. For the staggered rib roughened channel, as the increase of the Reynolds numbers from 1 500, 1 000, and 1 700 to 2 100, 1 500 and 2 200, the heat transfer enhancements are about 5.8—7.2 times, 4.2—5.4 times and 4.8—5.5 times for the ribbed channel with $S/e=10$, 15, and 5 , respectively. However, the increase of the heat transfer enhancements with the increasing Reynolds number from 3 000 to 6 000 in the turbulent region is far less than that in the laminar region. The largest heat transfer enhancements are about 6.5—7.5 times and 4.5—5 times for symmetrical and staggered rib channels with $S/e=10$, respectively. Especially for ribbed channel with $S/e=15$, there is almost no change for the heat transfer enhancement with the increase of Reynolds number. This indicates that the heat transfer enhancement effectiveness of ribbed channel in the laminar flow state is far higher than that in the turbulent state.

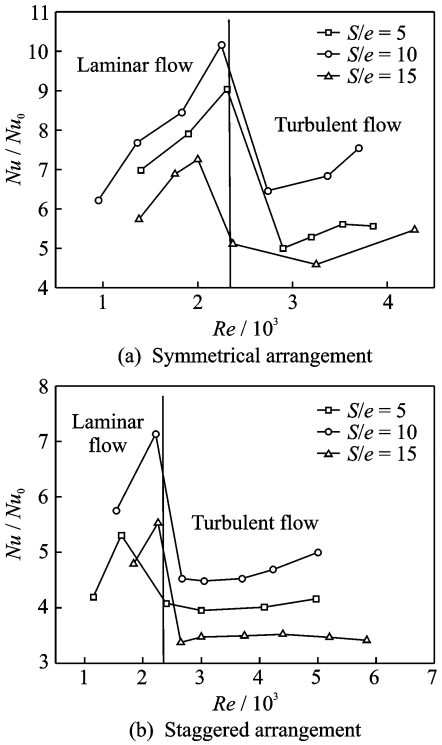

Fig. 8 Average Nusselt number ratio Nu/Nu_0 as a function of Reynolds number ($H/W=0.15$)

In order to analyze the heat transfer enhancement for the ribbed channel, the Nussult number of smooth channel Nu_0 must be obtained by an additional experiment in this paper. Fig. 9 shows the experimental results and empirical relation for the rectangular smooth channel of 180 mm (length) × 60 mm (width) × 15 mm (height) when the Reynolds number is increasing from 950 to 8 100. The empirical relation is $Nu_0=3.12+0.003Re$. At the same time, the comparison between the present experiment and the classical Dittus-Boelter correlation is also given in Fig. 10. As we can see from Fig. 10 that the difference between the present experimental result and the Dirttus-Boelter correlation result is very small, which proves the reliability of the experimental system.

Since the heat transfer enhancement in ribbed channel is typically accompanied by an increase in

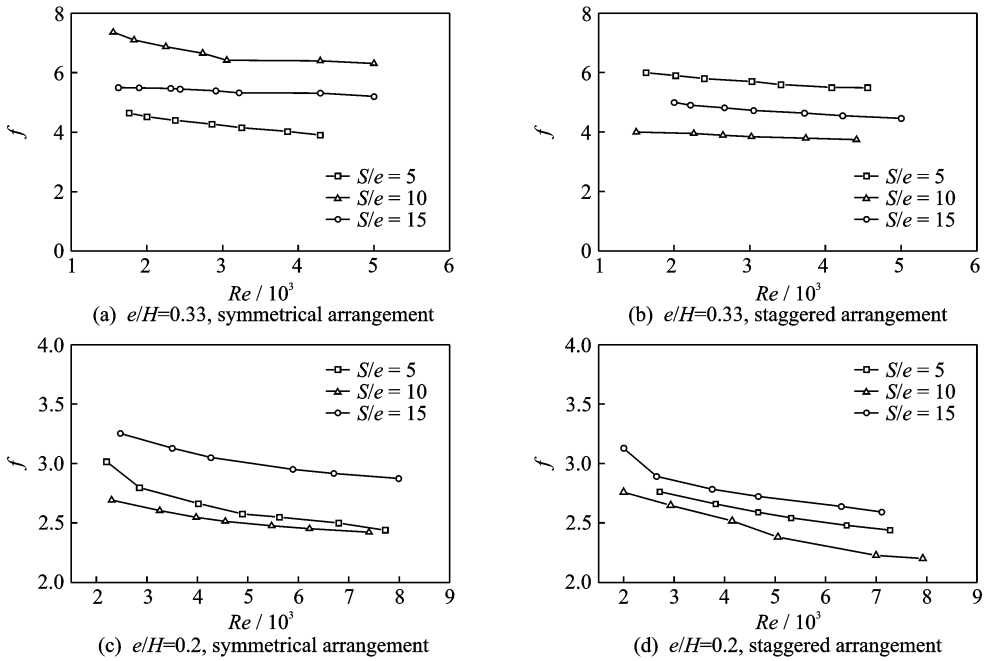

Fig. 9 Friction factor versus Reynolds number

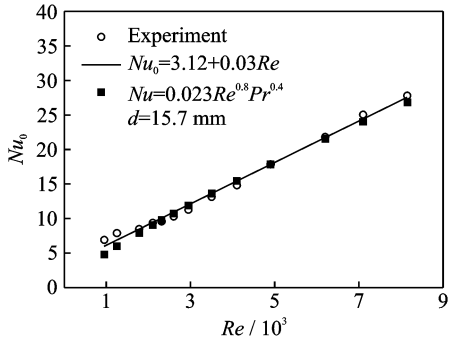

Fig. 10 Heat transfer coefficient of smooth channel

pressure drop, a comprehensive analysis of performance must include the effect of ribs on channel pressure drop. Fanning friction factor of the ribbed channels can be calculated according to Eq. (8). Fig. 9 shows the experimental results of the friction factor f in different ribbed channels. The friction factor, deduced from the experimental data, is depicted as a function of Re. It can be discovered that the friction factor is decreased gradually with the increase of Reynolds number. Whether symmetrical rib channel or staggered rib channel, the ribbed channel of $S/e=10$ corresponds to the largest friction factor, and the smallest fiction factor exists when $S/e=15$. At the same time, it can be seen clearly that the friction factor of the symmetrical rib channel is larger than that of staggered rib channel under the same S/e. The e/H also has a larger effect on the friction factor under the same rib arrangement. The fiction factor of $e/H=0.3$ is higher than that of $e/H=0.2$ under the same S/e. For example, for the symmetrical rib channel, when $S/e=10$, the largest and the smallest fiction factors of the rib channel of $e/H=0.33$ are 7.7 and 6.5, respectively, however, the largest and the smallest fiction factors of the rib channel of $e/H=0.2$ are 3.25 and 2.8, respectively. From above we know that the optimum heat transfer coefficient corresponds to the largest friction factor, and the minimum heat transfer coefficient corresponds to the smallest friction factor.

4 Conclusions

Heat transfer characteristics and pressure drop in rectangular rib roughened channels have been experimentally investigated by means of infrared thermography. Based on the results, the following conclusions are obtained:

(1) The rib pitch to height has a large effect on the heat transfer of the ribbed channel. The

effect of rib pitch to height ratio on heat transfer coefficient is not in a monotony increasing trend. The optimum pitch to height ratio in the experiment is 10.

(2) The rib arrangement has a larger effect on the heat transfer coefficient of rib-roughened channel. In general, the average Nusselt number of symmetrical ribs is higher than that of staggered ribs.

(3) A larger blockage ratio in the rib-roughened channel corresponds to a larger heat transfer coefficient. The heat transfer coefficient of blockage ratio $e/H=0.33$ is larger than that of blockage ratio $e/H=0.2$. The heat transfer coefficient of two-side rib channel is larger than that of one-side rib channel.

(4) The heat transfer enhancement effectiveness of ribbed channel in the laminar flow state is much higher than that in the turbulent state. The optimum heat transfer coefficient corresponds to the maximum friction factor, and the minimum heat transfer coefficient corresponds to the smallest friction factor.

Acknowledgements

This work was supported by the National Natural Science Foundation of China(No. 51276088).

References:

[1] LIOU T, HWANG J. Effect of ridge shapes on turbulent heat transfer and friction in a rectangular channel[J]. International Journal of Heat Mass Transfer, 1993, 36: 931-940.

[2] HAN J C, GLICKSMAN L R, ROHSENOW W M. An investigation of heat transfer and friction for rib-roughened surfaces[J]. International Journal of Heat Mass Transfer, 1978, 2: 1143-1156.

[3] TASLIM M E, LI T, KERCHER D M. Experimental heat transfer and friction in channels roughened with angled, V-shaped, and discrete ribs on two opposite walls[J]. ASME Journal of Turbomachinery, 1996,118: 20-28.

[4] KIM K M, LEE H, KIM B S. Optimal design of angled rib turbulators in a cooling channel[J]. International Journal of Heat Mass Transfer, 2009, 45: 1617-1625.

[5] ASTARITA T, CARDONE G. Convective heat transfer in a square channel with angled ribs on two opposite walls[J]. Journal of Experiment Fluids, 2003, 34: 625-634.

[6] TASLIM M E, LIU H A. A combined numerical and experimental study of heat transfer in a roughened square channel with 45-deg ribs[J]. International Journal of Rotating Machine, 2005, 1: 60-66.

[7] HAN J C. Heat transfer and friction characteristics in rectangular channels with rib turbulators[J]. ASME Journal of Heat Transfer, 1988, 110: 321-328.

[8] HAN J C, DUTTA S, EKKAD S V. Gas turbine heat transfer and cooling technology[M]. New York: Taylor & Francis, 2000.

[9] WAGNER J H, JOHNSON B V, HAJEK T J. Heat transfer in rotating passages with smooth walls and radial outward flow[J]. ASME Journal of Turbomachinery,1991, 113: 42-51.

[10] WAGNER J H, JOHNSON B V, KOOPER F C. Heat transfer in rotating passage with smooth walls [J]. ASME Journal of Turbomachinery,1991, 113: 321-330.

[11] HAN J C, ZHANG Y M, KALKUEHLER K. Uneven wall temperature effect on local heat transfer in a rotating two-pass square channel with smooth walls [J]. ASME Journal of Heat Transfer, 1993, 115: 912-920.

[12] BAILEY J C,BUNKER R S. Heat transfer and friction with very high blockage 45° staggered turbulators[R]. ASME GT2003-38611, 2003.

[13] HAN J C. Heat transfer and friction in channels with two opposite rib roughened walls[J]. ASME Journal of Heat Transfer,1984, 106: 774-781.

[14] JASON E D, DAVID G B, GUSTAVO A L, et al. Experimental measurements and computational predictions for an internally cooled simulated turbine vane with 90° rib turbulators[J]. ASME Journal of Turbomachinery,2012, 123: 42-51061005-1-8.

[15] FILIPPO C, MANFREDI S, TONY A. Experimental investigation of conjugate heat transfer in a rib-roughened trailing edge channel with crossing jets [J]. ASME Journal of Turbomachinery,2012, 134: 041016-1-11.

[16] XIE Gongnan, LI Shian, ZHANG Weihong, et al. Computational fluid dynamics modeling flow field and side-wall heat transfer in rectangular rib-roughened passages[J]. Journal of Energy Resources Technolo-

gy, 2013, 135(4): 042001.

[17] ZHENG Nianben, LIU Peng, SHAN Feng, et al. Effects of rib arrangements on the flow pattern and heat transfer in an internally ribbed heat exchanger tube[J]. International Journal of Thermal Sciences, 2016, 101: 93-105.

[18] TANG X Y, ZHU D S. Flow structure and heat transfer in a narrow rectangular channel with different discrete rib arrays[J]. Chemical Engineering and Processing: Process Intensification, 2013, 69: 1-14.

[19] MOON M A, PARK M J, KIM K Y. Evaluation of heat transfer performances of various rib shapes[J]. International Journal of Heat Mass Transfer, 2014, 71: 275-284.

[20] ZHANG Y M, GU W Z, HAN J C. Augmented heat transfer in triangular ducts with full and partial ribbed walls[J]. Journal of Thermophysics and Heat Transfer, 1994, 8(3): 574-579.

[21] KIML R, MOCHIZUKI S, MURATA A. Effects of rib arrangements on heat transfer and flow behavior in a rectangular rib-roughened passage: application to cooling of gas turbine blade trailing edge[J]. ASME Journal of Heat Transfer, 2001, 123: 675-681.

[22] STEPHENS M A, CHYU M K, SHIH T P, et al. Calculations and measurements of heat transfer in a Square Duct With Inclined Ribs[C]// Proceedings of the Joint Propulsion Conference and Exhibit. Lake Buena Vista, FL.:[s. n.], 1996: 1-3.

[23] SU G, CHEN H C, HAN J C, et al. Computation of flow and heat transfer in two-pass rotating rectangular channels(AR =1∶1, AR=1∶2, AR=1∶4) with 45-deg angled ribs by a Reynolds stress turbulence model[R]. ASME GT2004-53662, 2004.

[24] LIOU T M, CHANG S W, HUANG C Y, et al. Particle image velocimetry and infrared thermography measurements in a two-pass 90-deg ribbed parallelogram channel[J]. Journal of Heat and Mass Transfer, 2016, 93: 1175-1189.

[25] KIM D H, LEE B J, PARK J S, et al. Effects of inlet velocity profile on flow and heat transfer in the entrance region of a ribbed channel[J]. Journal of Heat and Mass Transfer, 2016, 93: 838-849.

[26] YANG Shiming, TAO Wenquan. Heat transfer [M]. Beijing: Higher Education Press, China, 2006.

[27] Yang Weihua, Liu Xue, Li Guohui, et al. Experimental investigation on heat transfer characteristics of film cooling using parallel-inlet holes[J]. International Journal of Thermal Sciences, 2012, 60: 32-40.

[28] HOLMAN J P. Experimental methods for engineerings[M]. New York: McGraw_Hill, 1984.

[29] HOLMAN J P. Heat transfer[M]. Beijing: China Machine Press, 2005.

Mr. **Xie Changtan** received his Master's degree in aerospace propulsion theory and engineering from Harbin Engineering University in 2011. He is now a senior engineer in AEEC Hunan Aviation Powerplant Research Institute, Zhuzhou. His research field is aero engine heat transfer and air system.

Mr. **Xue Shulin** received his Master's degree in aerospace propulsion theory and engineering from Nanjing University of Aeronautics and Astronautics in 2017. He is now an engineer in AEEC Hunan Aviation Powerplant Research Institute, Zhuzhou. His research field is aero engine heat transfer and air system.

Prof. **Yang Weihua** received his Master's degree in energy science and engineering from Harbin Institute of Technology in 1997 and Ph. D. degree from Shanghai Jiao Tong University in 2003. From 2003 to present, he has been working at College of Energy and Power Engineering of Nanjing University of Aeronautics and Astronautics. His research focuses on the research and application of spacecraft thermal protection technology.

(Production Editor: Sun Jing)